JOURNAL OF CATALYSIS 21, 1-11 (1971)

# 1-Butene Hydrogenation over Nickel(o)-Zeolite Catalysts

P. CHUTORANSKY, JR.* AND W. L. KRANICH

*Department of Chemical Engineering, Worcester Polytechnic Institute,*
*Worcester, Massachusetts 01609*

Received January 6, 1970; revised August 25, 1970

The vapor-phase hydrogenation of 1-butene, catalyzed by nickel supported on mordenite and Types X and A molecular sieve (0.19–9.8, 1.67 and 2.71 wt % Ni, respectively), was studied in the temperature range 40–135°C. Catalytic activity exhibited discontinuous behavior with temperature variation, as evidenced by transitions from one reaction region to another; abrupt changes in apparent activity by a factor of 10 to 100, or more were evident over narrow temperature ranges. The transition temperature and extent of discontinuity were found related to the overall activity level and the degree of dispersion of the active nickel component. In the high temperature region, hydrogenation and isomerization were consistent with Langmuir–Hinshelwood type mechanisms; adsorption effects were associated only with the butenes. Below the transition temperature a typical Arrhenius relationship was observed. A brief comparative study was also made of butene hydrogenation over palladium supported on mordenite. No abrupt transition from one reaction region to another was observed.

The use of molecular sieves as catalysts either by themselves or in conjunction with dispersed metals is of major industrial importance. In addition, because the sieve structure is better characterized than most catalyst systems, sieve-based catalysts are well suited for systematic studies of catalytic behavior.

In the present study, a relatively simple reaction, the hydrogenation of 1-butene, is investigated on a variety of catalysts consisting of nickel (and in a few cases palladium) deposited on molecular sieves. The effect of percentage nickel, the method of introduction of nickel, the dispersion of the metal and the structure of the zeolite is studied over a range of temperatures and feed compositions.

## NOMENCLATURE

| | |
|---|---|
| $k_{n\text{-butane}}$ | Hydrogenation rate constant for chemisorbed surface species (g-mole/min, g-catalyst) |
| $K_{\text{hydrogen}}$ | Hydrogen adsorption coefficient ($\text{atm}^{-1}$) |
| $K_{1\text{-butene}}$ | 1-butene adsorption coefficient ($\text{atm}^{-1}$) |
| $P_{\text{hydrogen}}$ | Hydrogen partial pressure (atm) |
| $P_{1\text{-butene}}$ | 1-butene partial pressure (atm) |
| $k_{2\text{-butene}}$ | Isomerization rate constant for chemisorbed surface species (g-mole/min, g-catalyst) |
| $k_{\text{eff}}$ | Effective hydrogenation reaction rate constant (g-mole/min, g-catalyst) |
| $P_{\text{butene}}$ | Total butenes partial pressure (atm) |

## CATALYST PREPARATION

Nickel catalysts were prepared by a conventional ion exchange of the zeolitic support with an aqueous solution of the nickel salt followed by reduction to the metallic state with gaseous hydrogen at 360–370°C. Prior to metal deposition, all zeolitic materials, mordenite (Norton trade name, ZEOLON) and Linde Types X and A, were in the sodium form, were powders

---

* Mobil Research and Development Corporation Paulsboro Laboratories, Paulsboro, New Jersey 08066.

and were of very high crystallinity. The chemical compositions and structural properties of these molecular sieves have been previously reported (*1–3*).

Ion exchange was conducted for two hours with nickel nitrate solution at 80°C. The solution was then filtered, and washed by agitation with a slightly acidic (pH 6) solution so that the nonexchanged nickel ions in the pores would not precipitate as the hydroxide. This procedure was repeated until a negative dimethylglyoxime test for the nickel ions was obtained in the filtrate.

An exchange with nickel ammine complex in place of nickel nitrate was conducted in a similar manner but with gaseous ammonia being constantly bubbled through the exchange solution to prevent decomposition of the ammine complex. A complete list of catalysts along with the exchange solutions and their concentrations and the resultant nickel loading is presented in Table 1.

In order to facilitate ease in handling, nickel-zeolite catalysts prepared in the powdered form were pelletized utilizing no binder and no filler. Approximately 5 $cm^3$ of powdered catalyst was placed in a 5/8-in. diameter mold with movable plugs in each end. The mold was placed in a Carrier hydraulic press and subjected to a pressure of 5000 psi. The resulting wafer was removed from the mold, broken and screened to obtain 6–8 mesh pellets. X-Ray diffraction analyses of the resultant pellets verified crystallinity retention; no structural degradation was observed. No catalyst powdering was experienced using these compression-type pellets.

TABLE 1
CATALYST PREPARATIONS AND CHARACTERISTICS

| Catalyst | Support material | Nickel crystallite size (Å) | Exchange temperature (°C) | Exchange time (hr) | Exchange solution |
|---|---|---|---|---|---|
| 9.8% Ni | Mordenite | 250 | 80 | 2.0 | 1.0N $Ni(NH_3)_6Br_2$ |
| 3.25% Ni(A) | Mordenite | — | 80 | 2.0 | 1.0N $Ni(NO_3)_2$ |
| 3.25% Ni(B) | Mordenite | 140 | 80 | 2.0 | 1.0N $Ni(NO_3)_2$ |
| 2.89% Ni | Mordenite | — | 80 | 2.0 | 0.099N $Ni(NO_3)_2$ |
| 1.45% Ni | Mordenite | 65 ± 15 | 80 | 2.0 | 0.024N $Ni(NO_3)_2$ |
| 0.19% Ni | Mordenite | too small to be determined | 80 | 2.0 | 0.001N $Ni(NO_3)_2$ |
| 1.67% Ni-X | Type X Sieve | 65 ± 35 | 80 | 2.0 | 0.024N $Ni(NO_3)_2$ |
| 2.71% Ni-A | Type A Sieve | 80 ± 40 | 80 | 2.0 | 0.038N $Ni(NO_3)_2$ |

Three palladium-mordenite catalysts were obtained from the Norton Company. These were: 2.0% Pd(A)-impregnated hydrogen mordenite; 1.9% Pd(B)-palladium exchanged sodium mordenite; and 1.89% Pd(C)-palladium exchanged ($NH_4^+$) hydrogen mordenite. Each was obtained in the form of 1/16-in. extruded pellets from which an organic lubricant was burned off in air at 350–400°C. Details of preparation were not made available.

## APPARATUS AND PROCEDURE

The studies were carried out in the continuous flow reactor with recycle described by Stauffer and Kranich (*4*). The apparatus was modified to incorporate a fluidized sand bed heating system for improved temperature control.

The purity of all reactants and the composition of products was determined by chromatographic techniques. The separation was carried out at 31°C on a 40-ft column of benzyl cyanide and silver nitrate on Chromosorb W (*5*). All butenes were of CP quality and were found to contain only trace impurities. In the analysis of the kinetic data, impurity concentrations were taken into account when determining the actual amount of reaction. No impurities were detected in the hydrogen feed.

Prior to evaluation, each catalyst underwent the following preparative sequence: Catalyst pellets were evenly distributed among 3/16-in. Pyrex spheres in the midsection of the 3/8-in. diameter reactor, the top and bottom inch of the 6-in. reactor being filled only with the Pyrex spheres.

A small sample of the catalysts charged to the reactor was calcined at approximately 1000°C. From the weight loss upon ignition, the weight of the catalyst charged to the reactor could be corrected to a bone-dry basis.

The loaded reactor was attached to the system and the catalyst dried and reduced *in situ*. After drying in a HPD nitrogen purge stream for 5–6 hr, using rapid heatup, a 24-hr reduction period at 360–370°C (50 $cm^3$/min hydrogen) was used for all catalysts. Recycle was utilized to minimize temperature gradients within the reactor during drying and reduction.

Upon completion of the activation-reduction sequence, the reactor temperature was reduced to 90°C. Each catalyst was subjected to a 10–12 hr reaction stabilization period with hydrogen and 1-butene flow rates of 100 and 50 $cm^3$/min, respectively.

In preliminary experiments it was established that gas flow rates were sufficiently high that bulk diffusion was not an important factor in determining reaction rate and that the stainless steel reactor system did not catalyze the chemical reactions of interest.

Catalytic activity and aging characteristics were determined by subsequent runs made in the following sequence of approximate temperatures: 90, 115, 135, 115, 90, 70, then at lower temperatures selected on the basis of catalytic activity, and finally again at 90°C, with catalyst purging with HPD nitrogen before each change to a new temperature level. With a fluidized sand bed for heat transfer and temperature control, coupled with the dispersion of the catalyst pellets within the bed, temperature gradients across the bed for any series of runs were less than 1–2°C, even at the highest conversion levels.

### MECHANISM STUDY—NICKEL MORDENITE

Although it was not the principal purpose of this study to establish a reaction mechanism, some effort was devoted to determining the types of Langmuir–Hinshelwood mechanism which are consistent with observed data. For this purpose low conversion runs were made over a wide range of feed compositions.

The main reaction, the direct hydrogenation of 1-butene, was well represented by the following kinetic expression for a typical 3.25% nickel-mordenite catalyst.

$$\text{Rate of hydrogenation} = \frac{k_{n\text{-butane}} K_{\text{hydrogen}} K_{\text{1-butene}} P_{\text{hydrogen}} P_{\text{1-butene}}}{1 + K_{\text{1-butene}} P_{\text{1-butene}}}.$$

This form of equation follows from a Langmuir–Hinshelwood mechanism in which butene adsorbed on one type of site reacts with either molecularly (dual-site) or atomically (triple-site) adsorbed hydrogen on a different type of site.

The nickel-mordenite catalyst–carrier system also catalyzed the isomerization of 1-butene to *trans*-2-butene and *cis*-2-butene. Slight traces of isobutylene and isobutane were also detected in the product stream. In the higher temperature regions studied, the isomerization reaction rate data were consistent with a Langmuir–Hinshelwood single-site surface-reaction-controlling mechanism.

$$\text{Rate of isomerization} = \frac{k_{\text{2-butene}} K_{\text{1-butene}} P_{\text{1-butene}}}{1 + K_{\text{1-butene}} P_{\text{1-butene}}}.$$

For hydrogenation, the 2-butenes appeared to possess approximately the same temperature and partial pressure dependencies as that for 1-butene, but were less reactive. The hydrogenation rate constants, and thereby the rates of hydrogenation, could be expressed as fractions of that for 1-butene. The rate of butane formation from *trans*-2-butene was about 0.24 times that from 1-butene, while that from *cis*-2-butene was about 0.37 times the rate from 1-butene. Typical results are shown in Fig. 1.

Although the data taken were too limited to allow positive identification of the reaction mechanism for either hydrogenation or isomerization, additional support for the mechanisms postulated is obtained from the fact that reasonably close values of the butene adsorption coefficient, $K_{1\text{-butene}}$, were calculated from the two independent analyses.

## High Conversion Studies

For ease of analysis and for a more direct comparison of experimental conditions with those encountered by catalysts industrially, most of the remaining studies were conducted at higher overall conversions (30–90%). Approximately the same feed rate and feed compositions were used for all runs. Even though the conversion was high, the concentration within the reactor varied but little because a high ratio of recycle to fresh feed was used in the reactor.

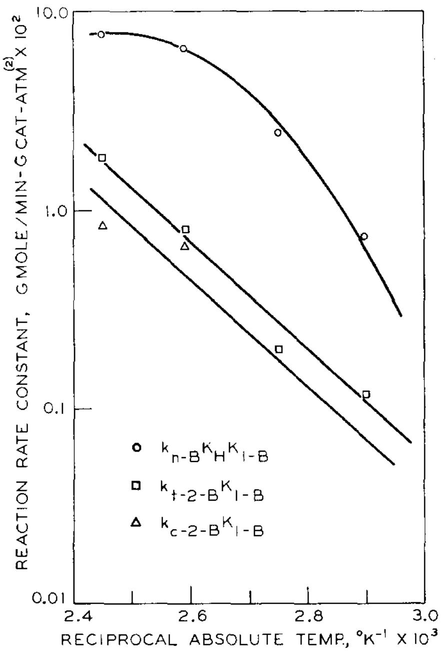

**Fig. 1.** Arrhenius plot of hydrogenation and isomerization rate constants (nickel-mordenite).

Under these circumstances a simpler kinetic expression was justifiable, in which the influence of the denominator in the Langmuir–Hinshelwood expression was considered to be small and the expression became first order in partial pressure of each reactant. On this basis an effective reaction rate constant, $k_{\text{eff}}$, was calculated from the data, described as follows:

$$\text{Rate of hydrogenation} = k_{\text{eff}}P_{\text{hydrogen}}P_{\text{butene}}.$$

Over a wide range of reactant partial pressures, $k_{\text{eff}}$ would itself be a function of $P_{\text{butene}}$ because of the Langmuir–Hinshelwood adsorption effect. For the results presented in this paper, however, experimental conditions were chosen such that the variation in reactant partial pressure was sufficiently small that $k_{\text{eff}}$ was essentially constant at any given temperature.

In this method of reporting results, no account is taken of the fact that hydrogenation of the 2-butenes resulting from isomerization of the 1-butene feed is much slower than that of 1-butene itself. All butenes are combined in calculating the partial pressure of butene and the $k_{\text{eff}}$ represents the rate of production of *n*-butane from all butenes. The values of $k_{\text{eff}}$ would, therefore, tend to be lower in the high conversion runs where 2-butene concentration is relatively high because of recycle, thus depressing the overall rate of hydrogenation.

Results are shown for several nickel-on-mordenite catalysts as a graph of log $k_{\text{eff}}$ vs $1/T$ in Fig. 2.

All of the curves show distinctly different behavior in a high temperature region from that in a low temperature region, separated by a well-defined transition temperature. Below the transition temperature a typical Arrhenius relationship was observed.

The transition from the high temperature region to the low temperature region was always accompanied by a large abrupt decrease in reactivity, frequently by a fac-

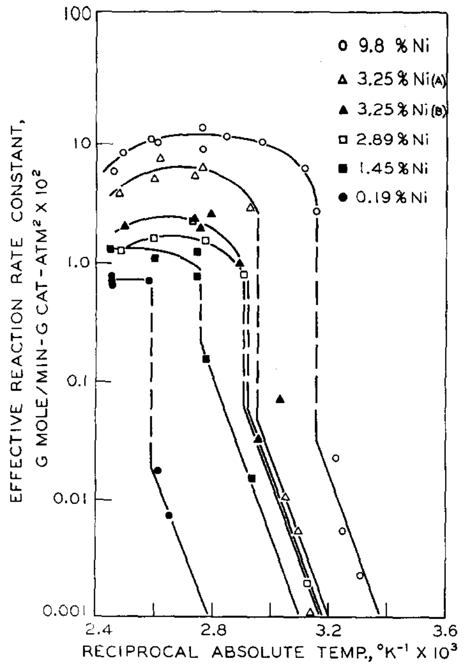

Fig. 2. Temperature dependence of effective hydrogenation reaction rate constants (nickel-mordenite).

tor of 10 to 100. Above the transition temperature as the reaction temperature was increased, the effective hydrogenation reaction rate constants gradually increased to maximum values which were approximately twice those just above the transition point and then decreased somewhat (30–40%). Below the transition temperature as the temperature was increased, the effective rate constant increased rapidly with an apparent activation energy of 30.5 kcal/g-mole for all catalysts.

The transition temperatures were dependent upon the amount of nickel loading and activity of the catalyst. For nickel-mordenite, the lower the activity, the higher was the transition temperature (Fig. 3). As the nickel content varied from 9.8 to 0.19% wt Ni, the transition temperature increased from 45 to 113°C.

The unusual temperature dependence of the activity of these catalysts can be plausibly though not incontrovertibly explained. Similar maximization and drop-off in activity at the high temperatures has been previously reported for hydrogenation over other supported nickel catalysts (*6–9*). The decrease in the adsorption equilibrium constant, $K_{\text{hydrogen}}$, leads to a starvation in hydrogen on the sites of the catalyst and a consequent decrease in reaction rate. If this is a true explanation, one would not expect to find a similar maximum in the same temperature region for isomerization activity since hydrogen is not involved. This is in fact shown in the hydrogenation and isomerization data of Fig. 1.

As the temperature decreases, the hydrogenation rate reaches a maximum, then begins to fall relatively slowly. This might be called the region of normal catalytic activity associated with Langmuir–Hinshelwood kinetics for surface reaction controlling.

According to the Langmuir–Hinshelwood mechanism, by far the largest fraction of active sites would be covered by butene (the most strongly adsorbed species). As the temperature falls, the fraction of butene-containing sites, at least those on the external zeolitic surfaces, increases, both because the reaction rate slows and removes the butene more slowly from both sieve and metal surfaces and because butene adsorption from the gas phase becomes more favorable. All active sites, internal and external, interact directly with the bulk gas phase reactants.

Over a short, rather well-defined temperature region the ports appear to become obstructed and the flow of materials by diffusion is markedly slowed. This may be thought of as clogging within the pores similar in effect to condensation, or as a bridging over the ports or mouths leading to the internal pores, either by butene or by a low-molecular-weight polymer of butene.

The simplest assumption would be that at a temperature similar to a boiling point, butene condenses within the pores. Because the pore dimensions are of approximately the same magnitude as the diameters of the reactant and product molecules however, the concept of a continuous condensed phase cannot be directly applied. The molecules within the inner pore structure interact with the molecular sieve surfaces more frequently and strongly than with the other adsorbed molecules. In addition, diffusion and equilibrium adsorption studies with mordenite (*16*) and Types X (*3*) and A (*1*) molecular sieves have shown that these phenomena are continuous functions of temperature in the range of this study.

The fact that the transition temperature, though sharp for any single catalyst, varies over a fairly wide range among the catalysts used, suggests that competing rate phenomena may be involved. In addition to hydrogenation and isomerization, a small amount of polymerization is occurring. The polymerized material diffuses outward more slowly than the monomer and therefore tends to block the passages or the ports. As reactivity for hydrogenation decreases, butene concentration on adsorbed sites increases, thus increasing the relative probability of polymerization. It is possible that over a short temperature range depending on catalyst activity, production and retention of polymer molecules may increase, thus choking off the flow of reactants and products. In a study of butene isomerization over modified mordenites, Kranich *et al.* (*10*) observed low molecular weight butene polymers during the outgassing of used catalyst.

Whatever the explanation, below the transition temperature region the effectiveness of the interior of the micropores appears to be choked off and the remaining activity results largely from the sites outside these pores.

The transition temperature is well defined because the pores in the molecular sieves are all of essentially the same dimensions. Below the transition temperature, if the hydrogen is to reach a vacant site or butane is to escape it must penetrate the blockage.

Because more rapid conversion of absorbed butene by reaction would tend to leave more open sites, it would be expected that more reactive catalysts would have lower transition (choking) temperatures. When relative activity is measured by behavior in either the high temperature or low temperature region, the curves of Figs. 2 and 3 are consistent with this concept.

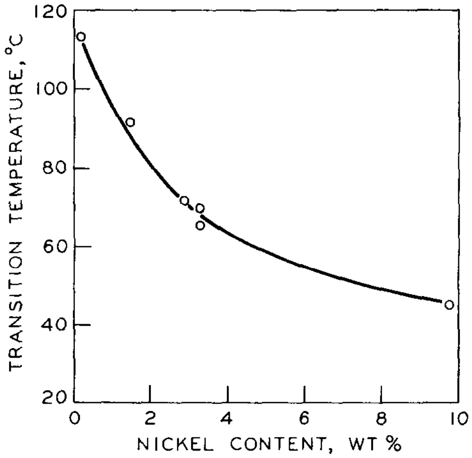

FIG. 3. Effect of nickel content on transition temperature (nickel-mordenite).

If a catalyst could bring sufficient hydrogen to the active sites, it might be expected that there would be no abrupt transition. For example, with palladium catalysts, such could occur due to the increased activity towards hydrogen chemisorption-activation and/or a different mechanism, such as that associated with the relatively free movement of hydrogen through the palladium mass. Carter *et al.* (*11*) observed that small amounts of platinum on alumina markedly enhanced the ease of removal of the adsorbed ethylenic species from the alumina during hydrogen treatment. They postulated the migration of reactive intermediates between the platinum and the alumina centers.

The removal of adsorbed complexes from an adsorbent or catalytic surface by admitting hydrogen has been accomplished with palladium and nickel films, as well as with supported platinum. However, the rate of removal with nickel was much slower than that for palladium. Bond (*12*) reported that, while 50–60% could be removed in 5 min with palladium at 0°C, with nickel only 20% was removed after 1 hr at 20°C.

To test the hypothesis that palladium catalysts might show different behavior with respect to transition temperatures, runs were made with three different palladium-mordenite pellets. Palladium-mordenite catalysts in fact showed no transition temperature but only a gradual decrease in activity with decreasing temperature over the range 140–50°C (Fig. 4). Although the hydrogenation of 1-butene over these palladium-mordenite extrudates was characterized by an apparent activation energy of 1.3 kcal/g-mole, indicating the probability of macropore diffusional influences, it still appears that the absence of any transitional behavior over this temperature range is due to the ability of the palladium to produce sufficient fluxes of activated hydrogen to react with and remove adsorbed butenes.

The shape of the two-region curves is similar to that experienced in solid-gas and or liquid-gas ignition phenomena and it might be proposed as an alternative explanation to the above that a similar mechanism exists here. At low ambient temperatures the catalyst mass would have a steady-state temperature only slightly above the ambient. Above the "ignition" temperature, however, the rate of removal of heat of reaction and the corresponding rate of supply of reactants might abruptly shift to a new steady-state value represented by a much higher particle (and reaction) temperature, as in a powdered coal flame. Calculations made by the method of Satterfield and Sherwood (*13*), however, indicate that this is an improbable explanation. Other calculations made by the methods of Weisz (*14*), and Roberts and Satterfield (*15*) showed an effectiveness factor for the conditions studied of approximately unity. In addition the ignition concept would not explain the observed variation in size of discontinuity nor the absence of bulk diffusion effects. The largely unknown mode of movement of molecules within the pores of sieves, however, leaves some uncertainty in any explanation.

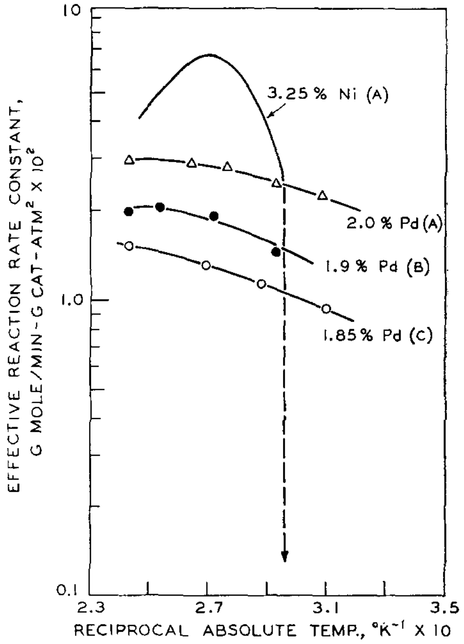

FIG. 4. Temperature dependence of effective hydrogenation reaction rate constants (palladium-mordenite).

In order to determine whether or not the transition temperature was real, reproducible and closely definable, the temperature was cycled several times for the 0.19% Ni-mordenite catalyst. The transition range, representing a 40-fold increase in activity, occurred repeatedly over a 4°C temperature variation (110–114°C). No significant dependence on the direction of approach to transition was observed.

## CATALYST DEACTIVATION

Two types of catalyst deactivation were observed, permanent and temporary. While the slower permanent deactivation definitely resulted in an irreversible loss of internal surface area, temporary (or reversible) poisoning could be readily removed by the overnight nitrogen purge between temperature levels. In addition, the most substantial deactivation occurred mostly at higher 1-butene partial pressures. Since all of the data reported herein were obtained at low 1-butene partial pressures with overnight nitrogen purges between runs, much of the intracrystalline surface area was always available for reaction.

To determine the extent to which carbonaceous deposits laid down during reaction might have rendered unavailable the catalyst pores, tests of properties were made before and after use. Available and accessible internal surface, as determined by water adsorption, corresponded very well with the observed permanent catalyst aging. For a typical coked catalyst (2.89% nickel-mordenite) water adsorption after simulated between-runs nitrogen purge was approximately 40% of the fresh catalyst; final activity was also approximately 40% of the initial value. Deactivation did not correlate with normal hexane adsorption; at this stage it exhibited 80% of fresh catalyst adsorption capacity. (Fresh catalyst water and *n*-hexane adsorption were 14 and 1.6 wt % respectively. Coke on catalyst was 4.8% by weight.)

## EFFECT OF NATURE OF SIEVE

For comparison with the mordenite-based catalysts, nickel-loaded catalysts on other sieves were also prepared and investigated. The 1.67 wt % nickel on Type X and the 2.71 wt % nickel on Type A molecular sieve catalysts were very much more active than the comparable nickel-mordenite catalysts. Arrhenius plots for nickel-X and nickel-A are shown in Fig. 5; 9.8% nickel-mordenite is also plotted for reference. Their kinetic and catalytic behaviors were essentially similar to those observed with the nickel-mordenites.

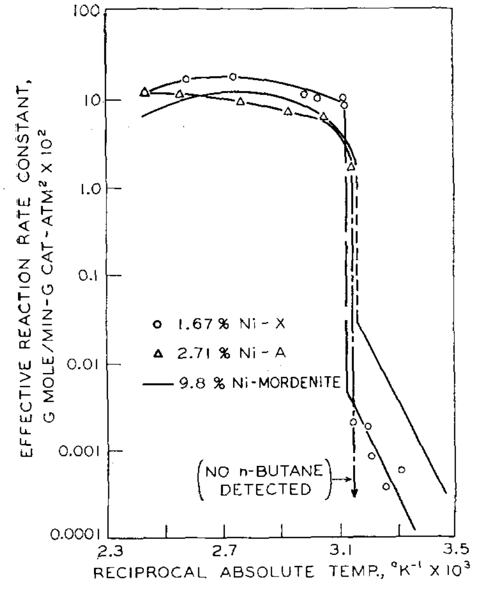

FIG. 5. Temperature dependence of effective hydrogenation reaction rate constants (nickel-X and nickel-A).

As the reaction temperature was decreased to below the transition point, the rate of reaction drastically decreased. For the nickel-X catalyst a 1–2°C temperature decrease at 46°C resulted in approximately a 1000-fold decrease in effective reaction rate constant. With the nickel-A catalyst a 10°C decrease at 44°C yielded such a significant decrease in reactivity that no butane product was detected in the product stream. The apparent activation energy of reaction in the low temperature reaction region with the nickel-X catalyst was the same as that observed for the nickel-mordenites. Thus it appeared that the same rate controlling mechanism was evident for both types of supported nickel catalysts in the low temperature region.

## EFFECT OF NICKEL CONTENT

Initially it was hoped that nickel loaded onto the sieves in various ways would show significantly different activity. It was hoped, for example, that exchanged nickel ions, would on reduction, yield more highly dispersed (and more active) nickel than that simply adsorbed or produced independently of the zeolite as from nickel carbonyl.

The results showed, however, that nickel atoms were sufficiently active and mobile during the processing steps that the bulk of the nickel accumulated into large agglomerates which must have been outside the micropores. Any special property of the freshly reduced, highly dispersed exchanged nickel was largely lost in the migration and agglomeration.

During the preparation of the exchanged catalysts, the nickel was introduced into the intracrystalline pore structure as atomically dispersed ions, their positions being fixed by the locations of the $AlO_4^-$ tetrahedra and electrical neutrality requirements. Once reduced to metallic nickel by hydrogen reduction at 360–370°C, the nickel atoms were no longer bound to the molecular sieve surface and were free to migrate and agglomerate into crystallites of metallic nickel. The presence of such nickel agglomerates was substantiated for all nickel-zeolite catalysts by their ferromagnetic properties, and electron spin resonance and X-ray diffraction patterns. The nickel crystallite sizes determined by X-ray diffraction techniques are presented in Table 1.

Although the mass average nickel crystallite sizes for nickel-X and nickel-A were 65 ± 35 and 80 ± 40 Å, respectively, it was still highly likely that a major portion of the catalytic activity could be attributed to a much larger number of small nickel crystallites, 4–30 Å, within the intracrystalline pore structure. For example, one large external 100 Å crystallite would have the same number of nickel atoms as one thousand 10 Å crystallite which would exhibit a much higher activity, even if only from surface area considerations. It was not unlikely that such small nickel crystallites were formed within the large cage-type cavities of the X- and A-type sieves. Once formed they would be too large to escape through the small 10 or 4 Å port windows, respectively. Thus many of these small nickel agglomerates, only a few angstroms in size, were thereby "trapped" within the cage type structure of the X- and A-type molecular sieves, yielding a higher degree of dispersion of the active nickel component.

However, formation of such trapped nickel agglomerates within the large parallel mordenite channels was less likely since the pore diameter was essentially uniform. The number of sites where stabilization of the intracrystalline nickel could occur was significantly lower than that for the cage-type structure of X- and A-type sieves. Therefore, much greater activities could be expected for the nickel-X and nickel-A catalysts as compared to the nickel-mordenite catalyst-carrier systems.

The 1.67 wt % nickel-X and the 2.71 wt % nickel-A hydrogenation catalysts exhibited approximately the same reactivity as did the 9.8% nickel-mordenite catalyst. This was probably at least in part due to a greater degree of dispersion of the active nickel component within the intracrystalline pores of the molecular sieve support.

The significantly greater decrease in reactivity of the X and A catalysts at the transition temperature (as compared with the nickel-mordenite systems) was further evidence of the relatively large amount of finely dispersed internal nickel. Although there was a possibility that Linde X and A molecular sieves were intrinsically more active than the mordenite as a result of catalyst-carrier interactions, the higher activity of the nickel-X and nickel-A catalyst was more probably due to the higher degree of dispersion of the active nickel component.

Nickel-X (1.67% Ni) and nickel-A (2.71% Ni), which were more active than their nickel-mordenite counterparts, possessed much lower transition temperatures (approximately 45°C). It should be noted that their activities were approximately the same as that for 9.8% nickel-mordenite, whose transition temperature was also 45°C. This agrees with the previous comments on the relationship between catalytic activity and transition temperature.

Nickel-mordenite catalysts were prepared over a wide range of nickel content in an attempt to determine a functional relationship between activity and loading.

If catalytic activity is to be correlated with nickel content, two distinctly different regions must be separately considered: (a) high temperature region where both internal and external nickel are available for reaction, and (b) low temperature region where activity is primarily due to external nickel crystallites.

For the nickel-zeolite catalysts in which the degree of dispersion of the active nickel component was the greatest, the change in reactivity at the transition temperature was most drastic. For example, 0.19% nickel-mordenite was found to be essentially inactive at 100°C, but at 114°C was a quite active hydrogenation catalyst (Fig. 2). Its high temperature activity was about half that of a 2.89% nickel-mordenite catalyst, showing a relatively high degree of dispersion of the active nickel component. Most likely, a high percentage of this nickel was supported within the intracrystalline pore structure of the mordenite. A 40-fold increase in reaction constant occurred over this 4°C temperature interval.

For 3.25% nickel-mordenite (A) which was merely a different batch of the same catalyst as 3.25% nickel-mordenite (B) and was prepared under supposedly identical conditions, a much greater degree of dispersion of the active nickel catalyst and a greater high temperature catalytic activity was observed with the former (A). Again, it was likely that much of this increased dispersion resulted in extensive amounts of metallic nickel within the intracrystalline pores of the mordenite. At the transition temperature, the decrease in activity was about 50-fold for the 3.25% nickel-mordenite (A) as compared to a 15-fold reduction with the less active (B) sample of the same catalyst material.

Because the effective $k$ in the high temperature region was so dependent on the degree of dispersion of the nickel, no single correlation with the nickel content was possible.

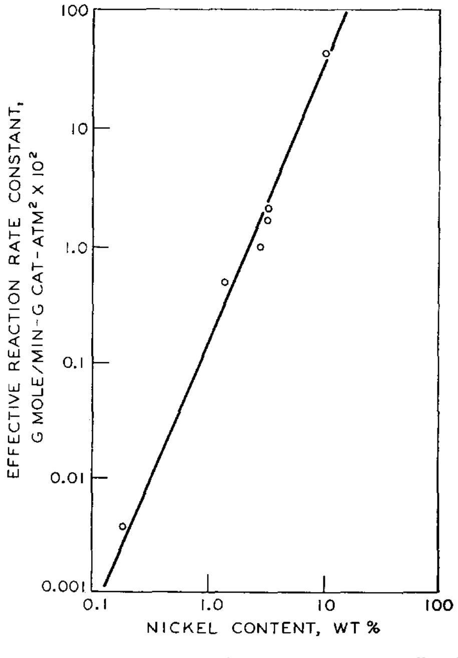

FIG. 6. Effect of nickel content on effective hydrogenation rate constants in the low temperature reaction region (nickel-mordenite).

In the low temperature region, the relative effective rate constants at an arbitrarily selected temperature of 85°C were obtained by extrapolation of the parallel straight lines of the Arrhenius plot (Fig. 2). These relative values are plotted (loglog) versus nickel content in Fig. 6. No correction for the degree of dispersion of the active nickel component was made.

A straight line relationship resulted in a good empirical correlation of the data. The slope of the best least-squares straight line was 2.5. Therefore, in the low temperature region

$$k_{\mathrm{eff}} \text{ (low temp region)} \propto (\%\mathrm{Ni})^{2.5}.$$

Because of the large number of unknown variables involved in the determination of the reaction rate constant in the low temperature region, no theoretical significance should be attached to this relationship.

## ACKNOWLEDGMENTS

Acknowledgment is made of analytical and financial assistance from the Norton Company, the Mobil Research and Development Corporation, the National Science Foundation and the Esso Educational Foundation.

## REFERENCES

1. BRECK, D. W., EVERSOLE, W. G., MILTON, R. M., REED, T. B., AND THOMAS, T. L., *J. Amer. Chem. Soc.* **78**, 5963–5971 (1956).
2. KEOUGH, A. H., AND SAND, L. B., *J. Amer. Chem. Soc.* **83**, 3536 (1961).
3. BROUSSARD, L., AND SHOEMAKER, D. P., *J. Amer. Chem. Soc.* **82**, 1041–1051 (1960).
4. STAUFFER, J. E., AND KRANICH, W. L., *Ind. Eng. Chem. Fundam.* **1**, 107 (1962).
5. *Book ASTM Stand.*, Part 7, 900 No. D1717-61T (revised 1961).
6. AMENOMIYA, Y., *Shukubai* **2**, 1–32 (1960); *Chem. Abs.* **55**, 3160 (1961).
7. HERKO, Cl., *J. Chem. Phys.* **47**, 454–473 (1950).
8. JENKINS, G. I., AND RIDEAL, E. K., *J. Chem. Soc.* **8**, 118 (1950).
9. TOYAMA, O., *Rev. Phys. Chem. Japan* **12**, 115 (1938).
10. KRANICH, W. L., MA, Y. H., SAND, L. B., WEISS, A. H., AND ZWIEBEL, I., Second International Conference on Molecular Sieve Zeolites, Worcester, Mass. (1970), Preprints **802–812.**
11. CARTER, J. L., LUCCHESI, P. J., SINFELT, J. H.,

AND YATES, D. J. C., *J. Amer. Chem. Soc.* **86,** 1494–1497 (1964); *Proc. Int. Congr. Catal. 3rd.* **1,** 644–653 (1965).

*12.* BOND, G. C., "Catalysis by Metals," pp. 232–233, Academic Press, New York/London, 1962.

*13.* SATTERFIELD, C. N., AND SHERWOOD, T. K., "Role of Diffusion in Catalysis," pp. 33, 37. Addison-Wesley, Reading, Mass., 1963.

*14.* WEISZ, P. B., "Appraisal of Effects of Mass and Heat Transport within Catalyst Pellets," Mobil Company Report, February 1961.

*15.* ROBERTS, G. W., AND SATTERFIELD, C. N., *Ind. Eng. Chem. Fundam.* **5,** 317 (1966).

*16.* FRABETTI, A. I., PhD thesis, Massachusetts Institute of Technology, Cambridge, Mass., 1965.